Proc. Natl. Acad. Sci. USA
Vol. 88, pp. 5202–5206, June 1991
Immunology

CD3η and CD3ζ are alternatively spliced products of a common genetic locus and are transcriptionally and/or post-transcriptionally regulated during T-cell development

(T-cell receptor/signal transduction/lymphoid differentiation/thymic selection)

LINDA K. CLAYTON*†, LUCIANO D'ADAMIO*†, FRANK D. HOWARD*‡, MONICA SIEH*, REBECCA E. HUSSEY*, SHIGEO KOYASU*†, AND ELLIS L. REINHERZ*‡

*Laboratory of Immunobiology, Dana–Farber Cancer Institute, and Departments of †Pathology and ‡Medicine, Harvard Medical School, Boston, MA 02115

Communicated by Robert C. Gallo, March 1, 1991 (received for review November 14, 1990)

ABSTRACT **The CD3η subunit of the T-cell receptor is thought to subserve an important role in signal transduction and possibly T-cell development. Herein we characterize the organization of the mouse CD3η gene and show that it is part of one gene locus that also encodes CD3ζ on chromosome 1. The NH_2-terminal sequence of CD3ζ and CD3η, which share the same leader peptide and are identical through amino acid 122 of each mature protein, is encoded by exons 1–7. However, exons 8 and 9 are differentially spliced to give rise to CD3ζ and CD3η: exons 1–8 encode CD3ζ and exons 1–7 plus 9 encode CD3η. RNase protection analysis with RNA from a variety of fetal, neonatal, and adult cell types indicates that expression of both gene products is T-lineage-restricted. Importantly, expression of CD3ζ and CD3η mRNA appears before or on day 16 of fetal gestation. Expression is apparently coordinate since no cell types tested express CD3ζ or CD3η alone. The steady-state level of CD3ζ mRNA is ≥40–60 times that of CD3η mRNA. In immature $CD4^+CD8^+CD3^{low}$ double-positive thymocytes and $CD4^+CD8^-CD3^{high}$ or $CD4^-CD8^+CD3^{high}$ single-positive thymocytes, the respective steady-state CD3ζ and CD3η mRNA levels are equivalent, whereas the amount of receptor-associated CD3ζ and CD3η proteins in double-positive thymocytes is ≈10 times less than in single-positive thymocytes. Nevertheless, the CD3ζ/CD3η protein ratio remains constant in all populations (40–60:1). Furthermore, discordance between mRNA and protein levels for CD3ζ and CD3η is also observed in splenic T cells. Thus, post-transcriptional and/or transcriptional regulatory mechanisms control CD3ζ and CD3η expression during T-cell development.**

The T-cell receptor (TCR) consists of at least seven distinct subunits (for review, see refs. 1–4). The Ti heterodimers are composed of α and β subunits that include variable domains responsible for antigen/major histocompatibility complex recognition by T lymphocytes. The CD3γ, CD3δ, CD3ε, CD3ζ, and CD3η subunits are invariant and are involved in TCR complex assembly and signal transduction. Whereas the CD3γ, CD3δ, and CD3ε subunits are encoded by related genes that are closely linked, the CD3ζ subunit is structurally (5) and genetically (6) distinct. Analysis of T–T hybridomas reveals that CD3ζ exists predominantly (>85%) as a 32-kDa homodimer within the TCR. However, a fraction of CD3ζ subunits (<15%) is complexed in a heterodimeric form with a 22-kDa subunit termed CD3η (7).

We have described (8) the primary structure of mouse CD3η as deduced from protein microsequencing and cDNA cloning. The NH_2-terminal sequences of CD3ζ and CD3η were shown to be identical through 122 amino acids of each mature protein but then diverged in the remainder of their respective COOH-terminal regions, consistent with alternatively spliced products of a common gene. Furthermore, the cytoplasmic domain of CD3η was shown to be 42 amino acids larger than that of CD3ζ, but to lack one of six possible tyrosine phosphorylation sites as well as a putative nucleotide binding site identified in CD3ζ (5). These structural features presumably account for the functional difference between CD3ζ and CD3η, including data suggesting that the CD3ζ–η heterodimer is important in coupling the TCR to inositol phospholipid hydrolysis (9) and may be linked to antigen-induced cell death in T-cell hybridomas (10). These findings suggest that CD3η is a component of a TCR isoform that plays an important role during thymocyte development. The present studies were conducted to define the anatomy of the CD3η gene and characterize CD3η expression during thymocyte development at both RNA and protein levels.

MATERIALS AND METHODS

Antibodies and Cell Lines. Rabbit anti-CD3ζ/η peptide antiserum 389 (11) was generously provided by R. D. Klausner (National Institutes of Health). A hamster–mouse somatic B-cell hybridoma, 145.2C11, producing 2C11, a monoclonal antibody (mAb) against mouse CD3ε (12), was generously provided by J. A. Bluestone (University of Chicago). MKD6, a mAb against mouse $I\text{-}A^d$, and M12.4.1 cells were generous gifts of L. Glimcher (Harvard School of Public Health, Boston). mAb J11D (13) and 500A2, a mAb against mouse CD3ε, were kind gifts from A. M. Kruisbeek (National Institutes of Health). Cell lines representative of day-14 and -17 fetal mouse thymocytes were derived by transformation with the retroviral construct J2 (14) and were also generously provided by A. M. Kruisbeek.

Genomic Library Screening and Restriction Mapping. The 1.9.2 library and 1.9.2 genomic DNA were the kind gifts of A. Winoto (Whitehead Institute, Cambridge, MA) (15). The Ar5 genomic library was provided by K.-N. Tan (Dana–Farber Cancer Institute) (16). BW5147 DNA was a gift of L. Glimcher; BALB/c, AKR, and B10.A(5R) spleen DNAs were from The Jackson Laboratory. Phage genomic libraries were screened using specific probes prepared by digesting pBS23 (CD3ζ) with *Eco*NI and *Eco*RI and pBS17 (CD3η) with *Ava* II and *Eco*RI (8). All probes were labeled by the random-priming method (17). Restriction mapping of the recombinant phage was performed as described (18) with *Bam*HI and *Hin*dIII enzymes. Mapping distances are accurate to within 100 base pairs (bp).

Analysis of Genomic and Phage DNAs. A 2-kilobase (kb) *Pst* I fragment of λZE3.20 hybridizing to a CD3η-specific oligonucleotide was subcloned into the *Pst* I site of pGEM-3zf- (Promega). Plasmid DNA was sequenced by the dideoxynu-

The publication costs of this article were defrayed in part by page charge payment. This article must therefore be hereby marked "*advertisement*" in accordance with 18 U.S.C. §1734 solely to indicate this fact.

Abbreviations: TCR, T-cell receptor; mAb, monoclonal antibody.

cleotide method (19). Oligonucleotide primers for sequencing were derived from the CD3η cDNA sequence and the SP6 and T7 promoters.

Phage and genomic DNAs were digested by *Bam*HI or *Hin*dIII, electrophoresed, and transferred to nitrocellulose (20). Probes for the genomic Southern blots were labeled (17) inserts of pBS23 (CD3ζ) and pBS17 (CD3η) encoding the entire cDNAs or oligonucleotides specific for CD3ζ exons 1–8 (6) and the unique CD3η sequence (8).

Preparation of Lymphoid Cell Populations. Single-cell suspensions of thymocytes and splenocytes were prepared from 4-week-old BALB/c mice (The Jackson Laboratory, or Taconic Farms, Germantown, NY). For splenic T cells, 6–7 $\times 10^8$ splenocytes were suspended in 6 ml of Hanks' balanced salt solution (HBSS) containing 5% (vol/vol) fetal calf serum and mixed with 2 ml of a culture supernatant containing mAb MKD6 and 200 μg of rabbit IgG directed against mouse IgG. To make splenic non-T cells, 3–4 $\times 10^8$ splenocytes were suspended in 5 ml of 10-fold concentrated 500A2 culture supernatant. For $CD4^+CD8^+CD3^{low}$ double-positive thymocytes, 5×10^8 thymocytes were suspended in 3 ml of 10-fold concentrated 500A2 culture supernatant. For $CD3^{high}$ single-positive thymocytes, 1.5×10^9 thymocytes were suspended in 7 ml of J11D culture supernatant as described (21). After an incubation on ice for 30 min, cells were collected by centrifugation, resuspended in 25% (vol/vol) rabbit complement (Cedarlane Laboratories, Hornby, ON, Canada) in HBSS containing 5% fetal calf serum and further incubated at 37°C for 30 min with continuous rotation. Dead cells were then removed by Ficoll/Paque (Pharmacia LKB Biotechnology) density centrifugation. After two cycles of the above procedure, 1.5×10^8 cells were recovered from each population. In general, purity of each cell population was ≈90% as assayed by expression of TCR, CD4, and CD8. Double-positive populations contained at most 10–20% double-negative cells. Fetal thymuses were obtained from timed-pregnant C57BL/6 mice (day 1 = day at which vaginal plugs were first observed) and kindly provided by A. M. Kruisbeek.

RNA Preparation and Analysis. pBSΔ17 was derived from the mouse CD3η cDNA clone pBS17 as follows: the *Sty* I–*Sma* I fragment of CD3η cDNA containing the 3′ 681 bp of exon 9 was excised from pBS17. The *Sty* I 5′ overhang was filled in with the Klenow fragment of DNA polymerase I and the linearized plasmid was ligated to obtain pBSΔ17. Antisense RNA was synthesized using T7 polymerase and 100 μCi (1 Ci = 37 GBq) of [^{32}P]UTP from pBSΔ17 linearized with *Acc* I. Hybridization to total cell RNA and RNase digestion were performed as described (22) and each sample was analyzed on a denaturing 5% polyacrylamide gel.

Immunoprecipitation and Western Blot Analysis of CD3ζ/η Proteins. Cells were lysed at 2×10^7 cells per ml in 1% digitonin lysis buffer [1% digitonin (Sigma) in 25 mM Tris·HCl, pH 8.0/0.15 M NaCl (TBS) containing 10 mM iodoacetamide, leupeptin (10 μg/ml), antipain (50 μg/ml), 1 mM phenylmethylsulfonyl fluoride, soybean trypsin inhibitor (10 μg/ml), aprotinin (10 μg/ml), and pepstatin (1 μg/ml) (all from Sigma)] by rotating at 4°C for 4 hr. The postnuclear supernatant from 2×10^8 cells was immunoprecipitated by rotating for 2 hr at 4°C with 50 μl of 2C11-coupled Sepharose CL-4B (4–5 mg/ml of bed volume). After extensive washing, antigen–antibody complexes were solubilized in 100 μl of nonreducing Laemmli's sample buffer at 100°C for 3 min. Samples containing 2×10^8 cell equivalents or 1:2 serial dilutions of an index sample were resolved by one-dimensional nonreducing SDS/PAGE in a 12.5% gel and transferred to nitrocellulose (23). Blots were probed with a 1:200 dilution of rabbit anti-CD3ζ/η peptide antiserum 389 followed by ^{125}I-labeled protein A (0.2 μCi/ml) as described (11). Autoradiography was at −70°C for 4 days on Kodak X-Omat AR x-ray film.

RESULTS AND DISCUSSION

Analysis of Genomic DNAs and Recombinant Phage Containing the CD3η Gene Segments. Genomic libraries from the mouse T–T hybridoma 1.9.2 and the Ar5 mouse T-cell clone were screened using CD3ζ- and CD3η-specific cDNA probes. Eleven phage carrying overlapping sequences were isolated. The restriction maps of 3 phage derived from the 1.9.2 library are shown in Fig. 1*A*. Restriction analysis using *Bam*HI and *Hin*dIII and hybridization with exon-specific oligonucleotide probes demonstrated that each phage contains CD3ζ exons 2–8 (6). In addition, phage λZE3.2 and λZE3.20 contain a CD3η-specific hybridizing fragment. Because CD3ζ exon 1 is known to be located >20 kb upstream of CD3ζ exon 2 (6), it is not surprising that all three phage lack exon 1. As indicated by Fig. 1*A* and shown in Fig. 1*B*, the sizes of the *Bam*HI and *Hin*dIII fragments containing exon 8 were different in each phage analyzed. Genomic DNAs derived from BALB/c, B10.A (5R), and AKR mice show an identical pattern and exon 8 is found on an invariant 4.6-kb fragment (Fig. 1*B*). PCR analysis on genomic DNAs and phage clones (data not shown) maps the site of variability to the intron between

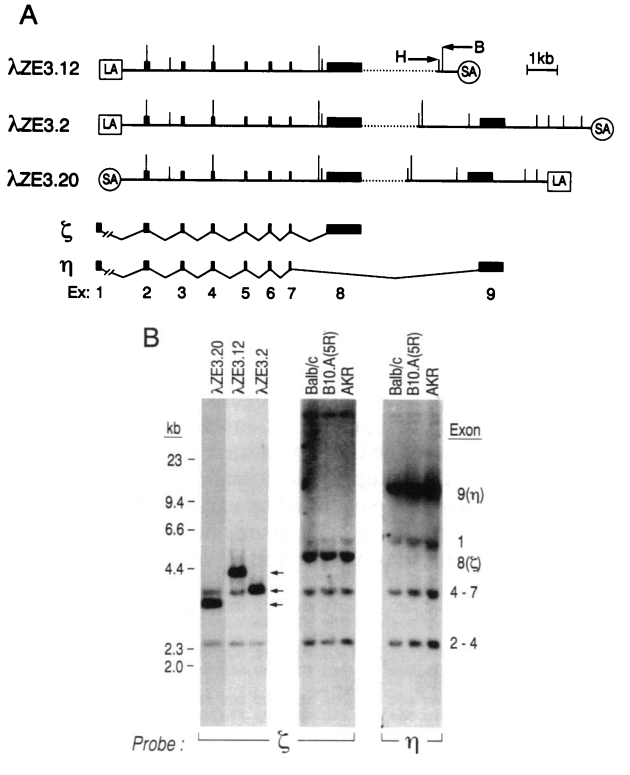

FIG. 1. Organization of exons 2–9 of the CD3ζ/η genomic locus. (*A*) Three recombinant genomic phage mapped for the CD3ζ/η locus are shown. Exon 1 is located >20 kb upstream of exon 2 (6) and is, therefore, absent from these phage. Exons are indicated by solid boxes. *Bam*HI (B) and *Hin*dIII (H) sites are indicated by long and short vertical lines, respectively. The dashed lines between exon 8 and the downstream *Hin*dIII site indicate variation in size of this fragment in the recombinant phage. SA and LA are the short arm and long arm of the λEMBL3 phage, respectively. The alternative splicing patterns of exons 1–9 giving rise to the CD3ζ and CD3η mRNAs are shown below the phage maps. (*B*) Southern blots of three recombinant λ phages and BALB/c-, B10.A(5R)-, and AKR-derived spleen DNAs digested with *Bam*HI and probed with CD3ζ (ζ) or CD3η (η) as indicated. Exons in the hybridizing *Bam*HI fragments of the phage are indicated by arrows; note that the exon 8 fragment comigrates with the fragment containing exons 4–7 in λZE3.2.

exons 8 and 9 (see Fig. 1). It appears that the latter region of DNA is altered upon passage in *Escherichia coli* during the recombinant phage cloning process. Based on the above analysis, we conclude that the actual size of the exon 8-containing *Bam*HI fragment is 4.6 kb. Thus, exons 8 and 9 are separated by ≈5.2 kb within the CD3ζ/η locus. Collectively, the physical maps of these phage (Fig. 1) are consistent with a previous report describing the intron–exon structure of the CD3ζ gene (6). The location of the CD3η-specific 5′ untranslated region is yet to be determined. More importantly, the data herein show that the CD3η gene is part of the same genetic region as CD3ζ.

Analysis of CD3η-Specific Coding and 3′ Untranslated Gene Segment. Sequence analysis of a 2-kb *Pst* I fragment of λZE3.20 revealed that the CD3η-specific portion (amino acids 123–185) is encoded by a single exon (Fig. 2). The genomic sequence is identical to that found in the CD3η cDNA (8) and consists of 782 bp encoding the unique portion of the CD3η protein as well as the entire 3′ untranslated region. A canonical splice acceptor site is present at the 5′ end of this exon (24).

Given the NH_2-terminal identity and COOH-terminal divergence of CD3ζ and CD3η sequences, we have suggested (8) that CD3η might be an alternatively spliced form of a gene encoding both CD3ζ and CD3η. The CD3η-specific exon was termed exon 9 to reflect the fact that CD3ζ and CD3η are part of the same genetic locus. Thus as predicted, CD3ζ and CD3η are products of alternatively spliced transcripts arising from a common locus as schematically depicted in Fig. 1*A*.

The CD3ζη Locus and Chromosome 1. CD3ζ has been mapped to mouse chromosome 1 (6) to a region that comprises a 6000-kb segment that is highly conserved between human chromosome 1 at 1q21–32 and distal mouse chromosome 1 (for review, see ref. 25) and also includes loci for a number of immunologically relevant genes (25–27) including the γ chain of the high-affinity IgE receptor (FcεRIγ) (28). This is of particular interest since a high degree of homology has been noted between the FcεRIγ and CD3ζ (29). Given the relatedness of CD3ζ and CD3η, this similarity in structure can be extended to CD3η and FcεRIγ. The organization of FcεRIγ and CD3ζη exons are analogous in several respects. (*i*) In each gene, exons 1 and 2 contain the leader peptide, the extracellular domain, the transmembrane region, and the first three residues of the cytoplasmic domain. (*ii*) The respective cytoplasmic domains are encoded by exons that are 21–81 bp long. The CD3ζ and CD3η cytoplasmic domains are encoded by three additional exons not found in FcεRIγ. Finally,

```
..tgtttcctcacaaacagGAC AGC CAC TTC CAA GCA GTG CAG TTC GGG AAC AGA AGA
                  Asp Ser His Phe Gln Ala Val Gln Phe Gly Asn Arg Arg

GAG AGA GAA GGT TCA GAA CTC ACA AGG ACC CTT GGG TTA AGA GCC CGC CCC AAA
Glu Arg Glu Gly Ser Glu Leu Thr Arg Thr Leu Gly Leu Arg Ala Arg Pro Lys

GGT GAA AGC ACC CAG CAG AGT AGC CAA TCC TGT GCC AGC GTC TTC AGC ATC CCC
Gly Glu Ser Thr Gln Gln Ser Ser Gln Ser Cys Ala Ser Val Phe Ser Ile Pro

ACT CTG TGG AGT CCA TGG CCA CCC AGT AGC AGC TCC CAG CTC TAA GGCCCTGTGCT
Thr Leu Trp Ser Pro Trp Pro Pro Ser Ser Ser Ser Gln Leu STOP

CAGCTCTGGTGATGACCCTGGCTGCTGTCACATGAGTTGTGGTGAGGATGGGACTTTTGAAAAATCTGATGT

TCCAATTTCTTTCATGCATGCTCTACTCAGAAGTGAGCAAGGGCCAAAACTCCTGGGCATGCATCTGAATGA

ATCTCTCAACTTAGAAAAGACTTGCCTGCCCCTCTGAGCTGGCCAGGTGTCCCCACCTACCCTTTGGCATGC

CTCCAAGTGCCAGGACGCCACAGACTGCATTGGGGCCGAAGACTTCCCTTTTCTTTGGTTTTTTTGTTTGTT

TTGAGTTTATACAATCATTAAGAAATCTTTGGTTTTGGCTGGAAATGGAAAAACAAAACAAATCAAAGAAAC

CACCCTCCCCTGGCTTATAGCAGCAGTATTATGACCTGACCTGGCTGAGCTTTCCCCCCCTCCAACTTTGGG

GGTGGAAATTGCAAGTTAAGAACTACATTCAAAGAAAACGTTGAAAGGGCCGGAGAAGCAGCTTCCAGAAAG

CCCGTCGGATATAAGATTGTCAAATAATAATAACTATTATTATAATATATTAATAATAAACTTAAATATTTG

GAAttctttttggtcat...
```

FIG. 2. Sequence of CD3η-specific exon 9 and flanking regions. Flanking regions are indicated by lowercase letters including the canonical splice acceptor site 5′ to exon 9 (lowercase letters). Exon 9 encodes the final 63 amino acids of the CD3η protein and the entire 3′ untranslated region of the CD3η mRNA. The polyadenylylation signal sequence is underlined.

significant amino acid homology exists between the region encoded by exon 2 of FcεRIγ and exon 2 of CD3ζη and between exon 5 of FcεRIγ and exon 8 of CD3ζ. In contrast, no COOH-terminal amino acid homology is apparent between FcεRIγ and CD3η. The similarities in exon–intron structure, sequence homologies, and chromosomal localization of FcεRIγ and CD3ζη suggest that gene duplication followed by insertion or deletion of three exons could explain the origins of these two genetic loci.

Analysis of CD3ζ and CD3η mRNA Expression. Prior studies demonstrated that thymocytes and peripheral T cells respond differently after TCR crosslinking; the majority of thymocytes do not proliferate and, in fact, die whereas T lymphocytes are triggered to proliferate (30, 31). Given the aforementioned structural differences in CD3ζ and CD3η proteins, it is possible that differential CD3η expression during thymocyte development is responsible for these signaling differences. To investigate this possibility through analysis of steady-state mRNA expression, we produced an antisense RNA probe to simultaneously detect and distinguish CD3ζ and CD3η mRNA in RNase protection assays (see Fig. 3*A*). This probe includes the junction between exons 7 and 9 in CD3η clone pBSΔ17 such that hybridization of CD3η mRNA results in a 173-bp protected fragment whereas CD3ζ mRNA protects a 100-bp fragment (Fig. 3*A*).

RNAs isolated from total adult and fetal mouse thymus, thymocytes, thymocyte subpopulations, v-*raf*/v-*myc*-retroviral-transformed fetal thymocyte lines, splenocytes, splenocyte subpopulations, liver, and brain were analyzed for CD3ζ and CD3η expression. As shown in Fig. 3 *B* and *C*, two major fragments protected by RNAs from T-lineage cells from BALB/c (Fig. 3 *B*, lanes 3 and 4, and *C*, lanes 1–5) or C57BL/6 (Fig. 3*B*, lanes 5–7) mice are observed at 173 and 100 bases. In contrast, no protected fragments are observed when the ^{32}P-labeled RNA probe was hybridized with BALB/c liver or BALB/c brain RNA (Fig. 3*B*, lanes 1 and 2) or splenic non-T-cell RNA (Fig. 3*C*, lane 6), demonstrating that both CD3ζ and CD3η mRNA are T-lineage-restricted. Consistent with this proposal is the observation that BALB/c kidney, B-cell lines A20 and M12.4.1, and the mast cell lines Cl.MC/57.1 (32) and IC2 (33) also lacked CD3ζ or CD3η mRNA, as judged by this protection analysis (data not shown).

To determine whether there were differences in CD3ζ and CD3η mRNA expression among different subpopulations of T-lineage cells, equal numbers of total thymocytes, $CD4^+CD8^+CD3^{low}$ double-positive thymocytes, and $CD4^+CD8^-CD3^{high}$ plus $CD4^-CD8^+CD3^{high}$ single-positive thymocytes, as well as total splenocytes and splenic T lymphocytes from 4-week-old BALB/c mice, were isolated. As shown in Fig. 3*C*, lanes 1–5, all populations expressed both CD3ζ and CD3η mRNA. Importantly, densitometry scanning of individual lanes showed that in each sample the CD3ζ-protected band was 20–30 times more intense than the CD3η band. Assuming that the intensity of these signals is proportional to the absolute amount of mRNA present and correcting for the ^{32}P content of the CD3η protected fragments, we conclude that the steady-state level of CD3ζ mRNA is 40–60 times greater than CD3η mRNA in each of the T-lineage-cell populations examined. Moreover, the steady-state amount of CD3ζ and CD3η mRNA is equivalent in double-positive and single-positive thymocytes but much lower in splenic T cells. Subsequently, CD3ζ and CD3η mRNA expression was examined during mouse gestation using RNAs obtained from C57BL/6 mice at days 18 and 16 of gestation (Fig. 3*B*, lanes 6 and 7) and newborn animals (Fig. 3*B*, lane 5). Again, all samples contained both protected fragments with similar CD3ζ/CD3η mRNA ratios. Similar results were obtained with RNA from thymi of C57BL/6 mice at 4, 8, 12, 28, and 42 days after birth (data not shown).

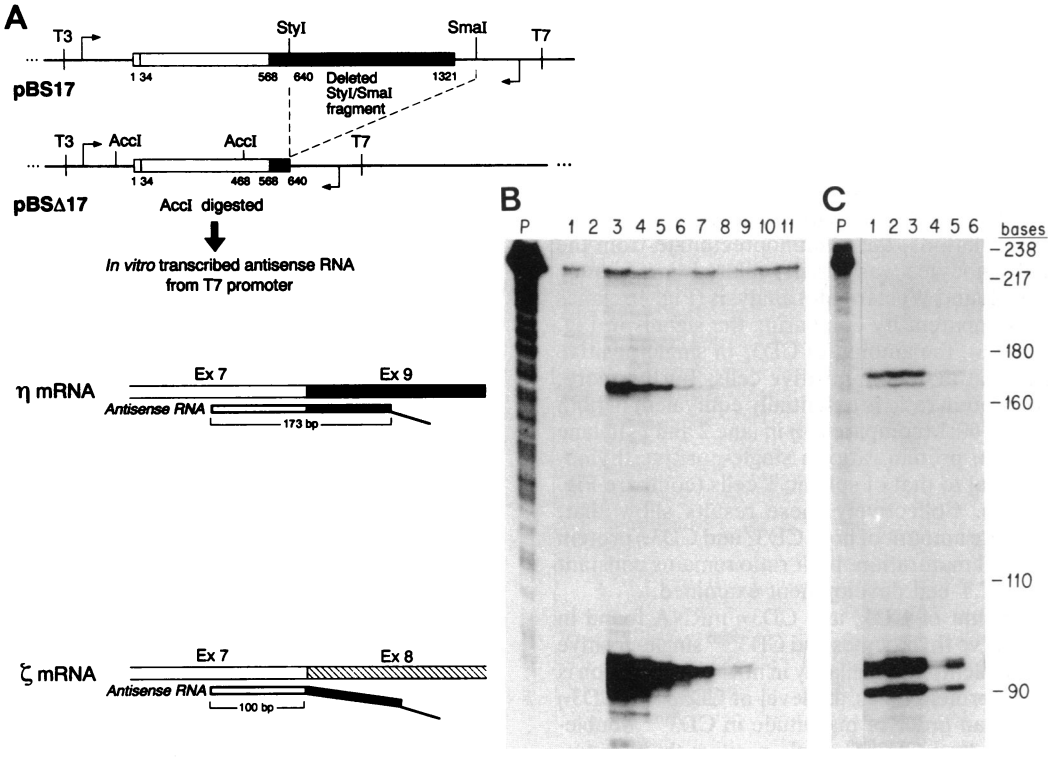

FIG. 3. Analysis of CD3ζ and CD3η mRNA expression using RNase protection. (*A*) CD3η cDNA clone pBS17 and its derivative pBSΔ17. Exon 9-specific sequence (bold line) and the CD3η-specific 5′ untranslated region (positions 1–34) (8) are indicated. The specific hybridization of CD3ζ and CD3η mRNA to the antisense RNA probe synthesized from pBSΔ17 are also indicated. Upon single-strand-specific RNase digestion, CD3ζ and CD3η mRNA protect 100 and 173 bases of the hybridized probe, respectively. The RNA analyzed in the RNase protection of the antisense probe (lanes marked P in *B* and *C*) are as follows: (*B*) Total RNA (15 μg) from liver (lane 1), brain (lane 2), newborn thymi (lane 5), day 18 (lane 6) and day 16 (lane 7) fetal thymi, day-17-fetal-thymus-derived clones C3H.B4 (lane 8) and C3H.B1 (lane 9), day-14-fetal-thymus-derived clones 35.1 (lane 10) and 32.1 (lane 11), and total RNA extracted from 8×10^7 (lane 3) or 4×10^7 (lane 4) adult thymocytes is shown. The band at ≈225 bases in each sample represents undigested probe. (*C*) Total RNA extracted from 3.75×10^7 adult thymocytes (lane 1), double-positive TCR^{low} thymocytes (lane 2), single-positive TCR^{high} thymocytes (lane 3), total splenocytes (lane 4), splenic T cells (lane 5), and splenic non-T cells (lane 6) is shown. The bands appearing just below CD3ζ and CD3η bands may be derived from overdigestion of the protected probe.

To examine CD3ζ and CD3η expression at a very early stage of thymocyte development, v-*raf*/v-*myc* retroviral transformants of day-14 fetal thymocytes were characterized. Two of the five representative clones, termed 35.1 and 32.1 ($CD2^+Thy\text{-}1^{low}PgP\text{-}1^{high}CD3^-CD4^-CD8^-$), are shown in Fig. 3*B* (lanes 10 and 11). Neither expresses CD3ζ or CD3η, suggesting that the CD3ζ/η locus is not transcriptionally activated until after this stage of gestation. Similarly derived transformants (C3H.B4 and C3H.B1) ($CD2^+Thy\text{-}1^{low}PgP\text{-}1^{high}CD3^-CD4^-CD8^-$) from day-17 thymocytes express both CD3ζ and CD3η (Fig. 3*B*, lanes 8 and 9). By assuming these cells are representative of normal thymocytes and in view of the results obtained with the day-16 fetal thymocytes (Fig. 4*B*, lane 7), transcription of the CD3ζ/η gene may begin on gestational days 15 or 16. The CD3ζ/CD3η mRNA ratio in these day-17 transformed clones (10–20:1) is lower than in normal T lymphocytes and thymocytes; the significance of this finding is unknown.

Analysis of CD3ζ and CD3η Protein Expression. To investigate how the above described quantitative differences in CD3ζ and CD3η mRNA levels among T-lineage subpopulations affected protein expression, portions of the thymocyte and splenic subpopulations prepared for RNA analysis as described above were examined for CD3ζ and CD3η protein expression by immunoprecipitation of the TCRs with anti-CD3ε mAb and subsequent Western blot analysis using an anti-CD3ζ/η heteroantiserum. As shown in Fig. 4*A*, the levels of both proteins increase during T-cell development. Thus, the amount of CD3ζ and CD3η proteins is lowest in $CD4^+CD8^+CD3^{low}$ double-positive thymocytes (lane 3) and highest in $CD3^{high}$ single-positive thymocytes (lane 2) and splenic T cells (lane 1). As expected, the total population of

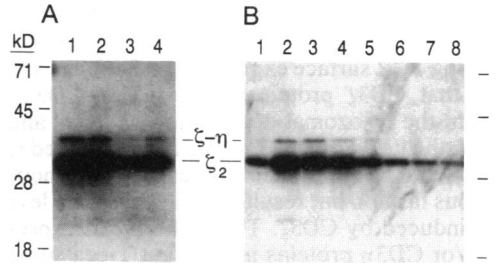

FIG. 4. Analysis of CD3ζ and CD3η proteins in thymic and splenic T-cell subpopulations. Digitonin lysates of the indicated subpopulations were immunoprecipitated with anti-CD3ε mAb 2C11 and examined by nonreducing SDS/PAGE followed by Western blot analysis using rabbit anti-CD3ζ/η peptide antiserum 389. CD3ζ/η protein–antibody complexes were detected by ^{125}I-labeled protein A. (*A*) Splenic T cell (lane 1), $CD3^{high}$ single-positive thymocytes (lane 2), $CD3^{low}$ double-positive thymocytes (lane 3), and total thymocytes (lane 4) are shown. Each lane contains material from 1×10^8 cells. (*B*) $CD3^{low}$ double-positive thymocytes (lane 1), $CD3^{high}$ single-positive thymocytes (lane 2), splenic T cells (lane 3), and serial 1:2 dilutions of $CD3^{high}$ single-positive thymocytes (lanes 4–8) are shown. Lanes 1–3 contain material from 1×10^8 cells. Lanes 4–8 contain material from 0.5, 0.25, 0.125, 0.06, and 0.03×10^8 cells, respectively. The positions of the CD3ζ–η and $CD3\zeta_2$ dimers are noted. Molecular mass standards (prestained) are bovine serum albumin (71 kDa), ovalbumin (45 kDa), carbonic anhydrase (28 kDa), and β-lactoglobulin (18 kDa).

thymocytes (lane 4) displays an amount of CD3ζ and CD3η protein intermediate between CD3^{low} double-positive thymocytes and CD3^{high} single-positive thymocytes. That the CD3ζ and CD3η proteins precipitated with the TCR represent the vast majority of these two proteins in the cell was demonstrated by sequential immunoprecipitation with anti-CD3ε followed by rabbit anti-CD3ζ/η antiserum (data not shown).

To more precisely compare the ratio of CD3ζ protein to CD3η protein between single-positive and double-positive thymocyte subpopulations, the immunoprecipitate from the single-positive thymocytes was serially diluted immediately prior to SDS/PAGE and Western blot analysis (Fig. 4*B*, lanes 2 and 4–8). As is apparent by comparing the signals in Fig. 4*B* (lanes 1, 5, and 6), the amount of CD3ζ in single-positive cells is $\approx$8 times that in double-positive cells. Furthermore, the CD3ζ/CD3η protein ratio is essentially equivalent in both cell types and is 40–60:1 (compare ζ–η in lane 2 and ζ_2 in lane 8). The CD3ζ/CD3η protein ratio in single-positive thymocytes is also identical to that of splenic T cells (compare Fig. 4*B*, lanes 2 and 3). Collectively these results show that, although the absolute amount of both CD3ζ and CD3η protein increases with T-cell maturation, their ratio remains constant during the stages of T-cell development examined.

Whereas the amount of CD3ζ and CD3η mRNA found in CD3^{low} double-positive thymocytes and CD3^{high} single-positive thymocytes is equivalent, this similarity in mRNA expression is not reflected at the protein level: the level of CD3ζ and CD3η protein is lower by an order of magnitude in CD3^{low} double-positive thymocytes than CD3^{high} single-positive thymocytes. This discordance is further evident in the splenic T-cell population, which expresses lower amounts of CD3ζ and CD3η mRNA than CD3^{low} double-positive thymocytes but contains substantially more of the corresponding proteins (Figs. 3*C* and 4). The observation that CD3ζ and CD3η mRNA levels decrease during T-cell maturation while CD3ζ and CD3η protein levels simultaneously increase implies that CD3ζ and CD3η expression is subject to post-transcriptional regulation. Furthermore, the stable ratio of CD3ζ to CD3η during maturation implies that such post-transcriptional regulation not only controls the absolute level of CD3ζ and CD3η protein but also maintains stringent control of the CD3ζ/CD3η protein ratio in the face of changing mRNA levels. These data show that CD3ζ and CD3η expression is transcriptionally and/or post-transcriptionally regulated during thymocyte development.

Implications. CD3ζ and CD3η proteins play important roles in controlling TCR surface expression. It has been shown, for example, that CD3ζ protein salvages Tiα-βCD3$\gamma\delta\varepsilon$ complexes from the lysozomal degradation pathway and routes the TCR to the cell surface (34). We have provided (23) data to suggest that CD3η protein is also capable of functioning in an analogous fashion but results in a TCR surface level lower than that induced by CD3ζ. Thus differential expression of CD3ζ and/or CD3η proteins in different T-cell subsets may control the surface level of TCR. The finding of post-transcriptional regulation of CD3ζ and CD3η proteins in double-positive TCR^{low} and single-positive TCR^{high} thymocytes is consistent with this view. Moreover, the levels of CD3ζ and CD3η proteins in these subpopulations correspond to the known differences in the copy number of cell surface TCRs in such subpopulations. Thus CD3ζ and CD3η protein levels may be responsible in part or in total for the observed surface TCR copy number difference. Presumably, the lower TCR expression in immature double-positive thymocytes necessitates a higher-avidity ligand interaction to activate thymocytes than would be required to activate thymocytes expressing high TCR amounts and as such may dictate a threshold for selection.

It has been proposed that CD3η is involved in signal transduction for negative selection in the thymus (10). If so, then one might have expected to find differential expression of CD3ζ and CD3η during thymic differentiation. Given that CD3ζ and CD3η mRNAs and proteins are expressed in T-lineage populations in both thymus and spleen, the similarities in the CD3ζ/CD3η mRNA ratios in all T-cell populations examined, and the increase in steady-state CD3η protein levels during T-lineage maturation, this proposal seems less likely. We cannot, however, rule out the possibility that CD3η may be preferentially expressed in a numerically minor subset of double-positive or single-positive thymocytes undergoing selection processes. In this regard development of CD3ζ- and CD3η-specific mAbs useful in immunohistochemical analysis may help to address this concern. However, definitive elucidation of the role for CD3ζ and CD3η in thymic development will likely result from studies utilizing transgenic strains of mice expressing purposefully altered levels of CD3ζ and CD3η and strains made devoid of CD3ζ or CD3η by targeted gene disruption.

1. Meuer, S. C., Acuto, O., Hercend, T., Schlossman, S. F. & Reinherz, E. L. (1984) *Annu. Rev. Immunol.* **2**, 23–50.
2. Clevers, H. C., Alarcon, B., Wileman, T. E. & Terhorst, C. (1988) *Annu. Rev. Immunol.* **6**, 629–662.
3. Davis, M. M. & Bjorkman, P. J. (1988) *Nature (London)* **334**, 395–402.
4. Ashwell, J. D. & Klausner, R. D. (1990) *Annu. Rev. Immunol.* **8**, 139–167.
5. Weissman, A. M., Baniyash, M., Hou, D., Samelson, L. E., Burgess, W. H. & Klausner, R. D. (1988) *Science* **239**, 1018–1021.
6. Baniyash, M., Hsu, V. W., Seldin, M. F. & Klausner, R. D. (1989) *J. Biol. Chem.* **264**, 13252–13257.
7. Baniyash, M., Garcia-Morales, P., Bonifacino, J. S., Samelson, L. E. & Klausner, R. D. (1988) *J. Biol. Chem.* **263**, 9874–9878.
8. Jin, Y.-J., Clayton, L. K., Howard, F. D., Koyasu, S., Sieh, M., Steinbrich, R., Tarr, G. E. & Reinherz, E. L. (1990) *Proc. Natl. Acad. Sci. USA* **87**, 3319–3323.
9. Mercep, M., Bonifacino, J. S., Garcia-Morales, P., Samelson, L. E., Klausner, R. D. & Ashwell, J. D. (1988) *Science* **242**, 571–574.
10. Mercep, M., Weissman, A. M., Frank, S. J., Klausner, R. D. & Ashwell, J. D. (1989) *Science* **246**, 1162–1165.
11. Orloff, D. G., Frank, S. J., Robey, F. A., Weissman, A. M. & Klausner, R. D. (1989) *J. Biol. Chem.* **264**, 14812–14817.
12. Leo, O., Foo, M., Sachs, D. H., Samelson, L. E. & Bluestone, J. A. (1987) *Proc. Natl. Acad. Sci. USA* **84**, 1374–1378.
13. Bruce, J., Symington, F. E., McKearn, T. J. & Sprent, J. (1981) *J. Immunol.* **127**, 2496–2501.
14. Rapp, U. R., Cleveland, J. L., Brightman, K., Scott, A. & Ihle, J. N. (1985) *Nature (London)* **317**, 434–438.
15. Winoto, A., Urban, J. L., Lan, N. C., Goverman, J., Hood, L. & Hansburg, D. (1986) *Nature (London)* **324**, 679–682.
16. Tan, K.-N., Datlof, B. M., Gilmore, J. A., Kronman, A. C., Lee, J. H., Maxam, A. M. & Rao, A. (1988) *Cell* **54**, 247–261.
17. Feinberg, A. & Vogelstein, B. (1983) *Anal. Biochem.* **132**, 6–13.
18. Rackwitz, H. R., Zehetner, G., Frischauf, A.-M. & Lehrach, H. (1984) *Gene* **30**, 195–200.
19. Sanger, F., Nicklen, S. & Coulson, A. R. (1977) *Proc. Natl. Acad. Sci. USA* **74**, 5463–5467.
20. Southern, E. (1975) *J. Mol. Biol.* **98**, 503–517.
21. Crispe, I. N., Shimokevitz, R. P., Husmann, L. A., Kimura, J. & Allison, J. (1987) *J. Immunol.* **139**, 3585–3589.
22. Melton, D. A., Krieg, P. A., Rebagliati, M. R., Maniatis, T., Zinn, K. & Green, M. R. (1984) *Nucleic Acids Res.* **12**, 7035–7056.
23. Clayton, L. K., Bauer, A., Jin, Y. J., D'Adamio, L., Koyasu, S. & Reinherz, E. L. (1990) *J. Exp. Med.* **172**, 1243–1253.
24. Breathnach, R. & Chambon, P. (1981) *Annu. Rev. Biochem.* **50**, 349–383.
25. Moseley, W. S. & Seldin, M. F. (1989) *Genomics* **5**, 899–905.
26. Siegelman, M. H., Cheng, I. C., Weissman, I. L. & Wakeland, E. K. (1990) *Cell* **61**, 611–622.
27. Knapp, W., ed. (1990) *Leukocyte Typing IV* (Oxford Univ. Press, Oxford).
28. Huppi, K., Siwarski, D., Mock, B. A. & Kinet, J.-P. (1989) *J. Immunol.* **143**, 3787–3791.
29. Kuster, H., Thompson, H. & Kinet, J.-P. (1990) *J. Biol. Chem.* **265**, 6448–6452.
30. Ramarli, D., Fox, D. A. & Reinherz, E. L. (1987) *Proc. Natl. Acad. Sci. USA* **84**, 8598–8602.
31. Smith, C. A., Williams, G. T., Kingston, R., Jenkinson, E. J. & Owen, J. J. T. (1989) *Nature (London)* **337**, 181–184.
32. Young, J. D.-E., Liu, C.-C., Butler, G., Cohn, Z. A. & Galli, S. J. (1987) *Proc. Natl. Acad. Sci. USA* **84**, 9175–9179.
33. Koyasu, S., Nakauchi, H., Kitamura, K., Yonehara, S., Okumura, K., Tada, T. & Yahara, I. (1985) *J. Immunol.* **134**, 3130–3136.
34. Chen, C., Bonifacino, J. S., Yuan, L. & Klausner, R. D. (1988) *J. Cell Biol.* **107**, 2149–2161.